

https://dspace.org/

Densification, microstructure and properties of liquidphase sintered silicon carbide materials

Can, Antionette

2006-02-06
http://hdl.handle.net/10539/172

Downloaded from a DSpace repository. https://dspace.org/

3. EXPERIMENTAL DETAILS

The details of the technique and experimental procedure are described in this section of the thesis. Note that there are two series of hot pressed materials: “HP-W” – initial hot pressing done at the University of the Witwatersrand, and “HP”- hot pressing done at the IKTS, based on experience of HP-W material production.

3.1 Raw materials and their characterisation

The powders were characterised using FESEM, XRD, Malvern Particle sizing, BET particle surface area and Leco oxygen content measuring equipment. The results of these measurements are recorded in Table 3.1.

Table 3.1 Particle sizing, surface area and oxygen measurement results for the powders used in the sintering

Powder	D(0.5) (μm)	BET surface area (g/m^2)	% O_2
UF15SiC	0.46	16.5	0.903± 0.016
AKP50 Al_2O_3	0.69	10.7	*
Y_2O_3- H.C. Starck	0.75	13.6	*

*not measured

The silicon carbide used was UF15SiC from H.C. Starck. An SEM image of the silicon carbide powder is shown in Figure 3.1. The silicon carbide powder consists of fine particles, which are agglomerated. The silicon carbide is a light brown, high purity powder (at least 99.9% pure). Impurities quoted by the manufacturer are aluminium (maximum 0.03 mass%), calcium (maximum 0.01 mass%) and iron (maximum 0.05 mass%)[69]. Rietveld refinement calculations in section 4.5 show that the silicon carbide consisted of 64.64±1.38 volume-% 6H polytype,2.54±1.4

mass-% 4H, 30.06±1.7mass-% 15R, 1.71±0.7 mass-% 3C (β) and 1.01±0.5 mass-% 2H polytypes.

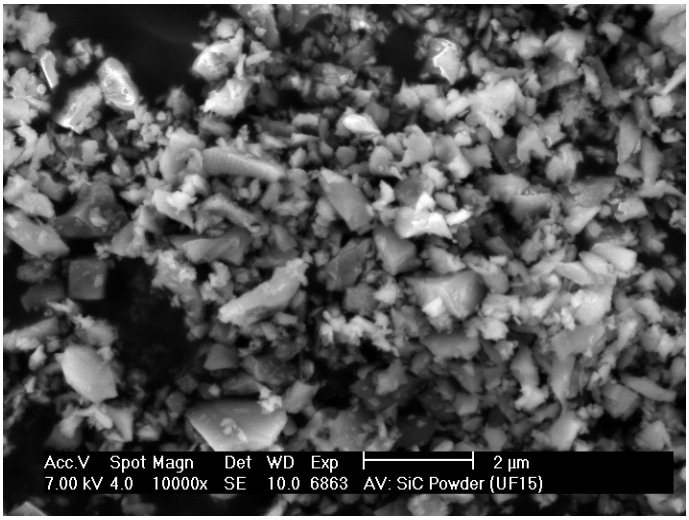

Figure 3.1 SEM micrograph of UF 15 silicon carbide powder (H.C. Starck)

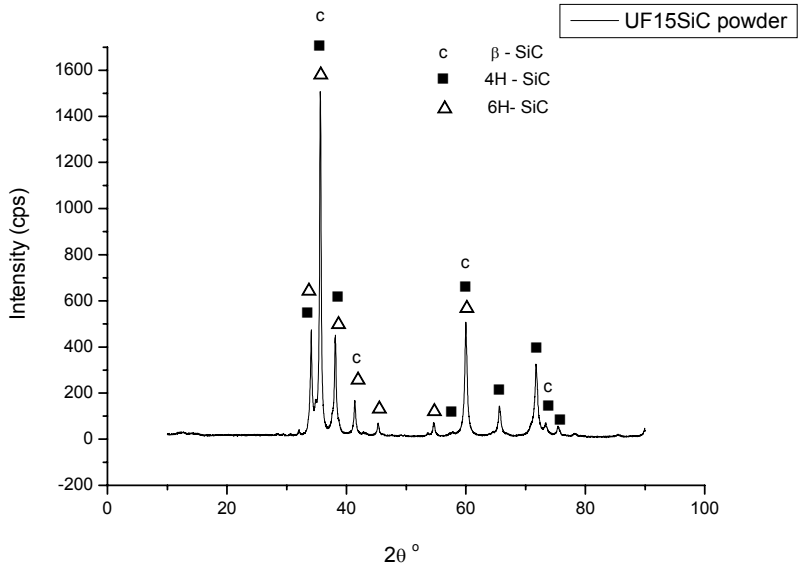

Figure 3.2 XRD pattern of the silicon carbide powder.

6H-SiC JCPDS file: 29-1128, 4H- SiC JCPDS file: 29-1127 and β– SiC JCPDS file: 29-1129

The sintering additives for the LPSSiC system in this project were yttria (Y_2O_3, grade C (fine) from H.C. Starck) and alumina (Al_2O_3, AKP50 from Sumitomo and A16 from Alcoa). FESEM micrographs of the yttria and alumina powders are shown in Figure 3.3 and 3.4 respectively. The yttria powder had a fine, flaky, white appearance. The alumina powder was also fine and white, but consisted of very fine “globular” (round) particles with a high tendency to agglomerate. This agglomeration tendency was also observed in the Malvern particle size distribution, where a peak was observed at 0.5 μm, and a second (smaller) peak above 10 μm. This second peak was most likely due to agglomeration of the particles measured in the Malvern particle sizing apparatus.

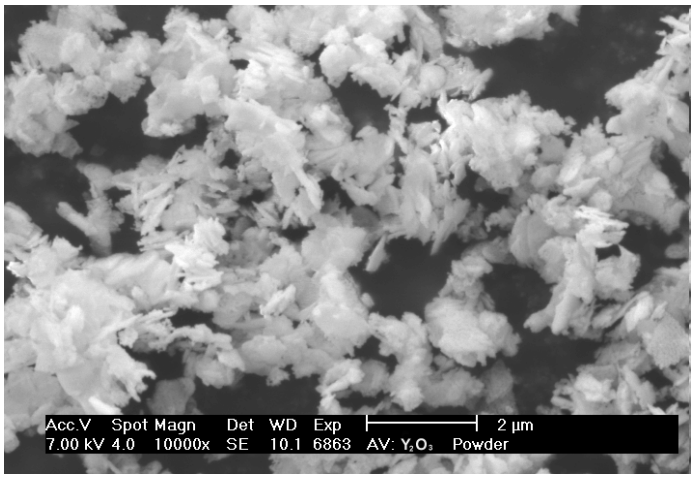

Figure 3.3 SEM micrograph of grade C yttria powder (H.C. Starck)

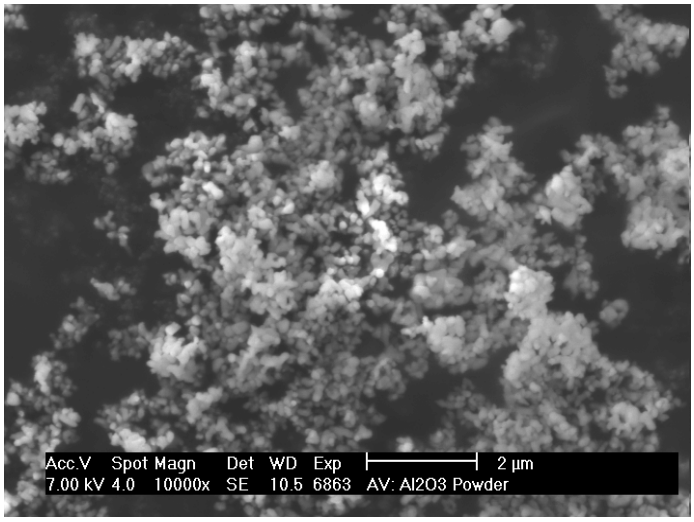

Figure 3.4 SEM micrograph of AKP50 alumina powder (Sumitomo)

3.2 Experimental apparatus

The details of the different equipment used to process and characterise the LPSSiC materials in this project are given in Table 3.2.

Table 3.2 Summary of experimental apparatus used

Function	Equipment details
Hot press- Wits University (HP-W)	TTI (Thermal Technologies Inc.) Astro, HP20 series (graphite interior, maximum 80 mm die)
Hot press-IKTS (HP)	HPW200/250, company KCE/FCT
Cold isostatic press	Company EPSI
Gas pressure sintering furnace	FPW220/300-2-2200-100-PFC, company FCT
Field Emission Scanning Electron Microscope (FESEM)	DSM982 Gemini, Fa. Zeiss
Energy dispersive X-Ray diffractometry (EDX)	Link ISIS EDX detector
Scanning Electron Microscope (SEM)	Stereoscan 260 Cambridge Instruments (Fa. Leica)
XRD – qualitative and Rietveld Quantitative phase analysis	* Qualitative- XRD 7 Seifert- FPM * Quantitative - Autoquan(Seifert FPM) (using the structural data given in the ICSD database).
Vickers hardness indenter	AVK 50 Schimadzu
Four-point bending strength	Type 8562 Instron
High temperature hardness	Laboratory equipment IKTS
Impedance spectroscopy	2-probe Novacontrol and 4-point Solartron 1610

3.3 Powder Processing

3.3.1 Preparation of powders for hot pressing in HP20 equipment (making HP-W materials)

The powders consisting of 90 mass-% UF15SiC and 10 mass-% of different mol ratios of Y_2O_3 and Al_2O_3, were mixed. The mixing was done in a suspension of isopropanol (Propan-1ol) as a dispersant, aided by the addition of 0.5 mass% triethylene glycol (Sigma- Aldrich, product number T5,9545-5) as plasticizer and 3 mass-% Triton-X (Sigma-Aldrich product number: 23, 472 -9) was added to act as a further de-agglomeration/ dispersant agent. The mixing operation was performed in a planetary ball mill in an alumina pot using ca. 10mm alumina milling balls.

The milling of the powder for hot pressing at Wits (HP-W) was performed with the parameters summarised in the Table 3.3 below.

Table 3.3 Table summarising milling parameters for HP-W materials

Milling apparatus	Planetary ball mill
Milling speed	220 rpm
Milling time	4 hours
Milling pot	250 ml Al_2O_3
Milling balls	ϕ 10mm Al_2O_3
Mass of milling balls	100 g
Total mass of powder	50 g
Mass of SiC	45 g
Dispersant (solvent)	140 ml Isopropanol
Organic binder	0.5mass% triethylene glycol
Additional dispersant	3.0 mass% Triton-X100 (Aldrich 23,472-9)

As seen in Table 3.4, which shows the alumina contamination in the HP-W material powders after milling, the alumina contamination was very high and therefore the milling parameter were adjusted for the milling done to produce powders for the second series of hot pressed, gas pressure sintered and ultra-high pressure sintered materials.

Table 3.4 Alumina contamination in HP-W materials

Aimed Composition (mol ratio)	Weight increase during milling (g)	Total Al_2O_3 (mass-%)	Total Y_2O_3 (mass-%)	Aimed Y_2O_3: Al_2O_3 mol ratio	Y_2O_3 : Al_2O_3 mol ratio after milling
$3Y_2O_3$: $5Al_2O_3$	0.6306	5.4860	5.6349	0.60	0.4638
$1Y_2O_3$: $1Al_2O_3$	0.7373	5.8588	6.6938	1.00	0.5159
$4Y_2O_3$: $2Al_2O_3$	1.4595	3.2682	8.0397	2.00	1.1107

After milling the suspension was dried in a "Rotavap" evaporator (under vacuum at about 60 ^oC). The powder was left an oven at 100^oC for a few hours to ensure that it was completely dry. The dried powder was sieved using a 212 μm sieve and only the material which passed through the sieve was used in further processing.

For preparation of the HP-W materials the powders were pressed using a 10 tonne uniaxial press. Approximately 8 grams of powder was pressed in a 20 mm diameter hardened tool steel die/punch set to obtain a green sample of approximately 8 mm height. Pressing was done by applying a load of 4 tons (pressure: 140 MPa). The green density of the samples was calculated to be, on average, 60%.

3.3.2 Preparation of powders for "HP" and "GPS" materials

Initially, the milling conditions as summarised in Table 3.5 were used for milling. A summary of all the milling experiments in sequence, for preparation of powders for HP and GPS and UHP sintering are summarised in Table 3.6 below.

After the first two experiments (in Table 3.6), and the high level of Al_2O_3 contamination observed there (shown in Table 3.6), the milling parameters, were changed to the parameters written in red in Table 3.5 below. The following changes were made. The total mass of powder to be milled in each pot was increased from 100g per pot, to 150 g, the mass of

milling balls was decreased, and the amount of milling dispersant solvent was also reduced slightly.

Table 3.5 Summary of milling conditions

Milling parameters	Initial milling conditions (experiments 1,2)	Optimised milling conditions (5 – 9)
Milling apparatus	Planetary ball mill	Planetary ball mill
Milling speed	200 rpm	200 rpm
Milling time	4 hours	2hours
Milling pot	250 ml Al_2O_3	250 ml Al_2O_3
Milling balls	ϕ 10mm Al_2O_3	ϕ 10mm Al_2O_3
Mass of milling balls	245 g	140 g
Total mass of powder	100 g	150 g
Mass of SiC	90g	135 g
Dispersant (solvent)	270 ml Isopropanol	240 ml Isopropanol
Organic binder	0.5mass% triethylene glycol	0.5mass% triethylene glycol
Additional dispersant	3.0 mass% Triton-X100	3.0 mass% Triton-X100

Table 3.6 Results of milling experiments for HP, GPS and UHP materials

No	**Sample**	**Mass Y_2O_3 (g)**	**Mass Al_2O_3 (g)**	**Milling time (hours)**	**Milling Al_2O_3 pick-up (g)**	**Corrected Y_2O_3/ Al_2O_3 mol ratio**
1	3Y:5Al Prelim1	5.71	4.29	4	11.97	1 : 6.4
2	4Y:2Al Prelim2	8.16	1.84	4	6.17	1 : 2
3	Test (4hrs) Prelim3	8.56	0	4	1.77	2.2 : 1
4	Test (2hrs) Prelim4	8.56	0	2	0.81	4.8 :1
5	3Y:5Al	8.56	5.69	2	0.81	1 :1.7 (3 : 5)
6	4Y:2Al	12.24	2.01	2	0.48	2.2 :1
7	1Y:1Al	10.33	3.92	2	0.49	1.1 : 1
8	4Y:1Al	13.48	1.02	2	0.49	4.0 : 1
9	1Y:4Al	5.35	9.15	2	0.87	1 :4.1

After successful milling experiments 3 and 4 in Table 3.6, the new milling parameters, as given in Table 3.5 were used and it was decided to rather use the 2 hour milling time. The amount of Al_2O_3 powder which was weighed into the pots for milling, was reduced to take into account the

Al_2O_3 which would be added to the mixture due to the low Al_2O_3 contamination from the balls. The powders which were prepared for the remaining hot pressing, gas pressure sintering and ultra-high pressure sintering experiments were done using the new milling parameters given in Table 3.5. Experiments No. 5 – 9 give the results of the milling experiments in preparation of the compositions for hot pressing and gas pressure sintering. After milling and drying of the suspension in a rotary evaporator, the powders were sieved through a 315 μm sieve for the remaining materials

The calculations for the additive volume percent (equation 3.1) and the theoretical density (equation 3.2) were carried out based on the rule of mixtures,

$$V_i = \frac{\frac{m_i}{\rho_i}}{\sum \frac{m_i}{\rho_i}} \times 100\%, \qquad (3.1)$$

where,

V_i = the additive volume percent of component I,

m_i = the mass-% of component I,

ρ_i = the theoretical density of component I,

i components were SiC, Y_2O_3, Al_2O_3 and SiO_2.

The results of the grain boundary phase volume calculations are given in Table 3.7.

The theoretical density of the sintered material, $\rho_{theoretical}$, was calculated according to the formula:

$$\rho_{theoretical} = \frac{\sum m_i}{\sum \frac{m_i}{\rho_i}} \times 100, \qquad (3.2)$$

where, ρ_{SiC} = 3.21,

ρ_{Al2O3} = 3.98,

ρ_{Y2O3}= 4.85,

ρ_{SiO2} = 2.33,

were used in the calculations.

The calculated theoretical densities are summarised in Table 3.7. $\rho_{theoretical1}$ in Table 3.7 and subsequent sections, is the theoretical density of the compositions, assuming Y_2O_3, Al_2O_3 and SiO_2 (always 1.7 mass% of the SiC powder), as making up the grain boundary phase. $\rho_{theoretical2}$ represents the theoretical density assuming that all SiO_2 has evaporated and the grain boundary consists of only Y_2O_3 and Al_2O_3.

Errors in the calculation of the theoretical density arise because these calculations are based on the rule of mixtures, assuming that the grain boundary phase of the sintered material consists of Y_2O_3, Al_2O_3 and SiO_2. In reality, these phases react during sintering and form the YAG or other phases with different densities (depending on the composition see section 4.2).

Table 3.7 Summary of the composition, volume content of the grain boundary phase and the theoretical densities of the materials prepared at IKTS

Composition	Molar ratio Y_2O_3:Al_2O_3	Mass ratio Y_2O_3:Al_2O_3	Volume grain boundary phase (%)	$\rho_{theoretical1}$ (g/cm^3)	$\rho_{theoretical2}$ (g/cm^3)
1Y4Al	1 :4.1	1 : 1.87	9.78	3.27	3.34
3Y5Al	3 : 5 (1:1.7)	1.32 : 1	9.34	3.28	3.35
1Y1Al	1.1 : 1	2.34 : 1	9.02	3.29	3.36
4Y2Al	2.2 : 1	4.92 : 1	8.84	3.29	3.37
4Y1Al	4.0 : 1	8.93 : 1	8.86	3.30	3.37

Note that the volume of the grain boundary phase in the sintered material will not be exactly as calculated because of some weight loss during

sintering (mostly loss of SiO_2, from the starting powder in the form of SiO gas and of Al_2O_3 in the form of the Al_2O gas.)

Powder for the series "HP" materials (hot pressed with HPW200/250), were not cold pressed before hot pressing.

3.3.3 Green sample preparation for GPS

The organic additives in the powders to be GPS were not burnt out until after green sample preparation. These powders were weighed into an elastic rubber "bag", which was evacuated. While the air was being sucked out, the compact increased in hardness, and the powder was formed (using a tile), to get a rectangular bar of dimensions ca. 10 cm X 2cm X 2cm.

Three more "rubber bags" were then wrapped over the samples and they are then cold isostatically pressed, in oil, at 250 MPa, prior to gas pressure sintering.

3.4 Burning out organic additives

Organic additives triethylene glycol (0.5 mass-%) and Triton X-100 (3 mass-%) were burnt out of the green cold pressed HP-W samples and the powders for the HP series. This burning out was done in an open-air furnace at 450°C for 1 hour (with a ramping cycle of 5°C/minute up to 450°C and then allowed to cool rapidly after a one hour burning out.)

In the case of the cold-isostatically pressed bars for gas pressure sintering, organic additives were removed by a cracking procedure (a non-oxidation removal of organic species from the green sample) at 1100°C in an Ar atmosphere. This process only removed 2.8 mass-% of the organic additives, leaving 0.7 mass-% in the materials. With this procedure, there

was likely to be more carbon left in the green sample, compared to burning out in air. This is because of the lack of oxygen to react with the carbon and remove it as carbon monoxide and carbon dioxide.

The presence of any remaining carbon is not detrimental to the processing of the liquid-phase sintered silicon carbide ceramic, since it reacts with the SiO_2 layer around the SiC particles to form SiC, as shown in equation 3.3. This is beneficial to the sintering process.

$$SiO_2 + 3C = SiC + 2CO. \qquad (3.3)$$

One experiment was done where a sample, a $1Y_2O_3{:}4Al_2O_3$ composition bar, was cut in half and half of it was burnt out at 450°C in air (the same as the burning out procedure for the HP materials) and the other half was burnt out at 1100°C in argon. The result of this experiment is shown in Table 4.3 (in section 4.1) showing only minor changes.

3.5 Densification and post-sintering heat treatment

3.5.1 Hot Pressing (HP)

Firstly, the hot pressing of the "HP-W" materials and then of the "HP" materials will be discussed in this section.

The sintering program that was used to prepare HP-W materials is summarised in Figure 3.5. At 1500°C the load was gradually increased from ca. 300 kg to 1100kg (36MPa) at a rate of approximately 80 kg per minute during a 10 -minute holding period. After sintering the load was gradually decreased at 1500°C, at a rate of approximately 150 kg per minute.

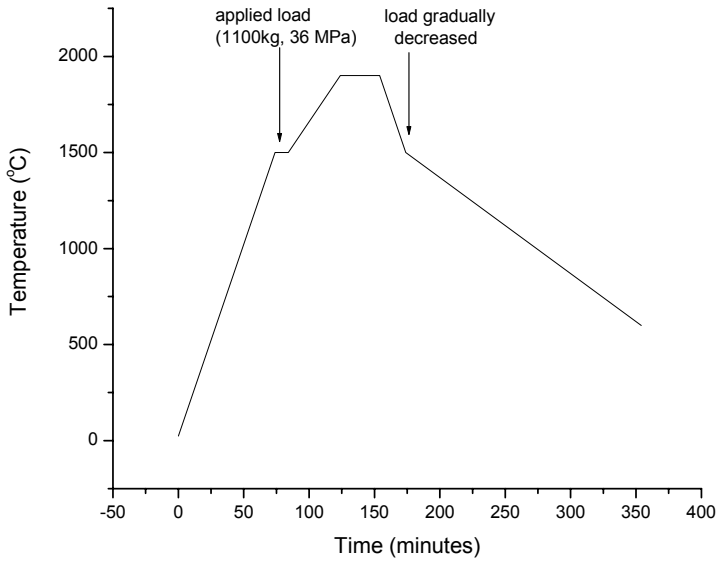

Figure 3.5 Hot pressing sintering program for HP-W materials

The first hot pressing was done at Wits University, using a program as described in Figure 3.5. A number of practical problems were encountered and experiments were done to solve these problems. The holding (sintering) temperature and time were varied, to decide which would be the best conditions for the preparation of the "main" materials to be analysed further in this research, i.e. optimised. The optimisation experiments, done with the $1Y_2O_3$:$1Al_2O_3$ composition, are summarised, in Table 3.8.

Table 3.8 Summary of different sintering temperatures and times attempted in HP-W experiments (all for 10mass%, $1Y_2O_3$:$1Al_2O_3$ sintering additives)

Sintering temperature (°C)	Sintering time (hours)
1800	1
1850	1
1900	1
1900	0.5

The HP-W samples were sintered in graphite pots (SGL Carbon, grade R 812). See the schematic diagram of the graphite pots and die-punch in Figure 3.6.

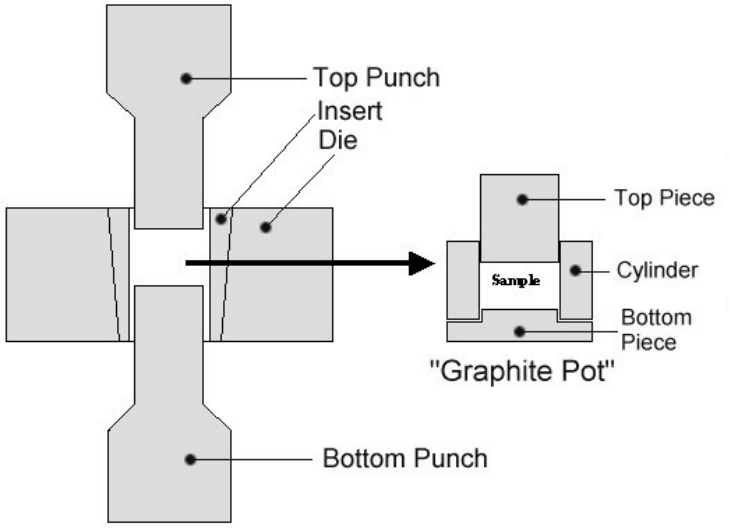

Figure 3.6 Die-punch system for hot pressing of HP-W materials

The graphite pots and die insert and punches were cleaned with acetone, and placed in an oven at 110°C to dry and heat them for the next step. A mixture of hBN, polyvinylpyrollidene ("PVP") and water was kept stirring on a magnetic stirrer plate. The graphite pot pieces and die insert and punches were individually removed from the oven and one by one painted with the hBN suspension, using a small (5 mm diameter) paint brush, while hot. The samples were heated first to speed up the evaporation of water. All of the pieces were placed in the oven again after painting, to ensure that they completely dry before assembling the system for hot pressing.

The cold pressed green samples, as described in section 3.3, were then placed in the coated graphite pots. The die-punch system, with the green sample in the graphite pots, was placed into the hot press. After sintering, the bottom and top pieces of the graphite pots could be removed with

reasonable ease. However, the cylindrical part used had to be sawed in three places, and the sample knocked out, breaking the edges of the sample. This was assumed to be necessary due to some reaction between the sample and the graphite (despite the hBN suspension coating.) Evidence of some kind of reaction was the gold-coloured residue observed between the sample and the graphite.

Dense materials were obtained for experiments at 1800 ^{o}C, 1850 ^{o}C, 1900 ^{o}C (1hour sintering, 36 MPa), as well 0.5 hour sintering at 1900°C. Three compositions were then sintered at 1900°C, under 36 MPa for 0.5 hours, using the same sintering cycle as in Figure 3.5, for systematic characterization in the project.

For the hot pressing of the "HP" materials (and gas pressure sintering), powder from the last 5 compositions in Table 3.6 (experiments 5 -9) was used.

For the hot pressing of the HP materials, the powders were poured into a graphite insert, 80 mm in diameter, which had also been coated with hBN. The punch- die- insert system used was similar to that shown in Figure 3.6. The insert was inside a die and there were two cylindrical graphite pieces on either side of the powder in the insert. The samples were sintered at 1925°C, under 30 MPa for half an hour.

All the HP-W and HP samples were sand-blasted and ground flat before undergoing Archimedes density measurements (three times for each sample). The temperature was measured on the outer surface of the die using pyrometer. From earlier investigations it is known that the temperature inside the die is 50- 70 °C lower than what is measured.

3.5.2 Gas Pressure Sintering

Pre-sintering preparation of the sintering environment is very important in this technique of sintering. This is because of high weight losses of the materials (discussed in section 2.6.3) during extended periods of heat treatments, particularly under low pressure.

The sintering "system" used consisted of three large graphite pots (diameter 250mm). The preparation involved the following: All three pots were painted with a LPSSiC suspension. The bottom and top pots were filled with "dummy" LPSSiC samples. The middle pot, contained the materials to be gas pressure sintered.

Because of the problem of decomposition reactions in the Y_2O_3-Al_2O_3-based LPSSiC system, in the literature[39, 40, 92, 96,111,150,153] often powder beds are used to combat the mass loss from the samples. This is however not always effective, and it is not a very good practical solution since the powders tend to "stick" to samples. To combat mass loss in gas pressure sintering and post-sintering heat treatments, the samples were put in small graphite pots, inside a larger graphite pot, with extra pots of dummy LPSSiC samples in the furnace above and below the samples sintered and heat treated. Qualitative explanations for these practical actions are outlined below.

The influence of the effective furnace volume or exactly the ratio of volume of the solid to gas can be demonstrated using the following:
For an ideal gas at a fixed temperature and pressure:

$$\left(\frac{V}{V_m}\right)_{pT} = n, \qquad (3.4)$$

where,

V is the effective volume of gas in immediate sintering environment of the samples in the furnace;
V_m is the molar volume of the gas at the given temperature and pressure in the furnace, (at room temperature and pressure 22.4 dm^3 for an ideal gas);
n is the number of moles of gas in the furnace; and
p and T are partial pressure and temperature in the furnace respectively.

The effective volume of the furnace is the sintering environment that the samples are in contact with, which includes the space not occupied by solid. By reducing the effective volume of the sintering environment, V is reduced, which will reduce the number of moles of gas in the sintering environment, i.e. the number of moles of gas which would be released from the dummies and the samples. For this reason, the samples were gas pressure sintered and heat treated in small graphite pots, which were placed in a larger closed graphite pot with LPSSiC samples. The small graphite pots were closed, minimizing diffusion through them. For calculations in equation 3.4, a volume between that of the small pots and bigger pots should be used.

The use of dummy LPSSiC samples during the sintering causes the evaporation of Al_2O, SiO from both the samples and the dummies to be reduced, but does not change the partial pressures, i. e. the overall amount of the evaporating components. This allows thermodynamic equilibrium of reactions (2.7) and (2.8) (repeated below) to be reached by less mass loss of the actual samples. Being packed into containers above and below the samples, the dummies had a higher free surface exposed to the surrounding volume of the furnace, i.e. the dummy pots tend to seal the actual pot in a relatively small volume.

The CIPed samples were gas pressure sintered for 60 minutes at 1925°C under a gas pressure of 80 bar (8MPa) using the cycles summarised in Table 3.9.

Table 3.9 (also 4.2): Gas pressure sintering cycles used

Cycle	Mean heating rate (K/min)	Holding time at 1875°C	Starting gas pressure (bar)
A	5	30	1
B	10	30	1
C	5	60	1
D	10	60	2

The mass of each sample was measured before and after sintering to determine the mass loss associated with reactions 2.7 and 2.8. Mass loss and Archimedes density measurement were used to determine the success of the sintering experiment. The results of these experiments are discussed in detail in section 5.1. Cycle A was successful in densifying the four lower Y_2O_3 content compositions, although densification of the GP4Y2Al composition was not as reproducible as the other, lower Y_2O_3-content compositions. Cycle C and D were attempts to improve the densification of the two higher Y_2O_3-content materials (GP4Y2Al and GP4Y1Al). These attempts were not successful and are discussed in section 5.1.

Cycle A was therefore used to sinter the GPS samples for systematic characterization in this project.

3.5.3 Ultra-high pressure sintering

The powders were weighed into metallic cups of 50 mm diameter and an overlapping, close-fitting second cup was pressed to cap the first cup, using a uniaxial press. The encapsulation was electron beam welded closed and the metal-encapsulated powder unit was assembled with other parts in a larger capsule to be placed in the ultra-high pressure sintering

belt furnace. The larger capsule assembly is similar to that shown in Figure 3.7. Two samples were sintered in one larger capsule (assembled unit, shown in Figure 3.7) per ultra-high pressure press run.

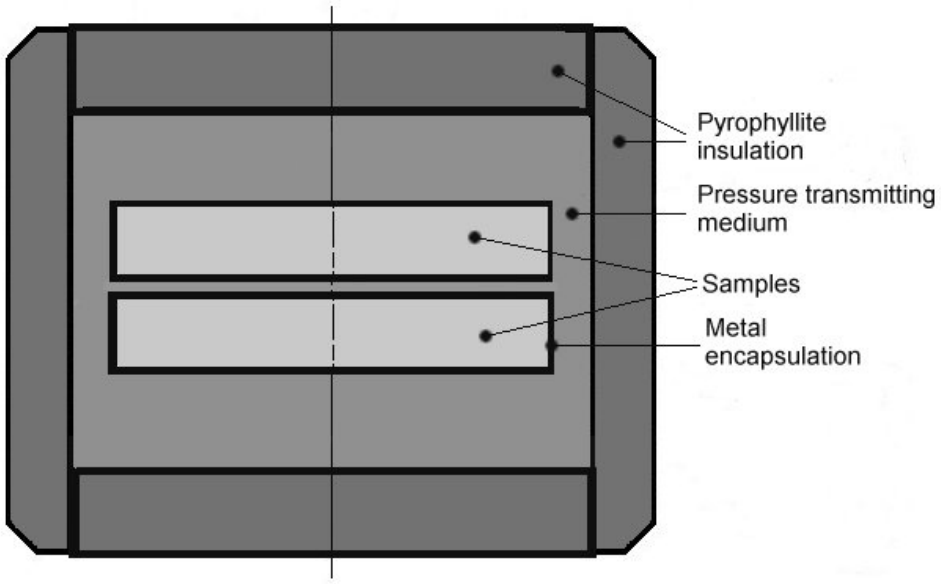

Figure 3.7 Schematic diagram to show encapsulation similar to what was used to ultra-high pressure sinter two samples at a time. Similar to capsule used by Gadzira *et al.* [22].

Experiments were done to optimise the running conditions. In these optimisation experiments one 4mass-% and one 20 mass-% sintering additive powder system were sintered together in one larger capsule for each run. The experimental conditions are shown in Table 3.10.

Table 3.10 Ultra-high pressure optimisation sintering experiments

RUN no.	Approximate temperature* (°C)	Cooling
1	1500	Very fast
2	1550	Very fast
3	1550	Slower
4	1550	Even slower

* exact temperature unknown because furnace power-controlled

The success of the sintering was judged by looking at how "solid" the sintered sample was, degree of cracking and density. The best results were obtained with the run number 3, and therefore this was used to sinter the four main compositions of this project for more systematic analysis. After sintering the metal encapsulation was ground off.

The density of the UHP materials was measured using the Archimedes method. Squares (18mm by 18mm) were cut (from the three main UHP compositions) for the purpose of impedance spectroscopy measurement, and small pieces suitable for polishing and crushing for XRD analysis were also cut.

3.5.4 Post- sintering heat treatments

Post-sintering heat treatment experiments of HP-W materials were done under flowing argon. A heat treatment of the three compositions was done at 1900 ^{o}C, in the hot press (HP20) furnace for 2 hours. The samples were placed in a powder bed of coarse silicon carbide, in a graphite pot placed in the furnace. Mass loss and density was measured after heat treatment. An additional heat treatment was done on the $1Y_2O_3$:$1Al_2O_3$ HP-W material at 1700 ^{o}C for 2 hours.

For the heat treatment of the HP and GPS materials, the experimental "set-up" for the heat treatments was identical to that of the gas pressure sintering (described in 3.5.2). The post-sintering heat treatments were done in the gas pressure sintering furnace under an argon gas pressure of 80 bar (8MPa). The program used for heat treatment was similar to Cycle A used for gas pressure sintering, except that the heating rate was slightly faster (average 15K per minute) and there was no intermediate holding time at 1875°C.

After heat treatment the HP materials were cut into squares (21 X 21 X 6) mm, suitable dimensions for electrical measurements. The GPS material bars were cut into slices, with approximate dimensions (20 X 20 X 6) mm. Three heat treatment experiments were carried out at 1925°C: 1.5 hours, 5 hours and 8 hours. One heat treatment was also carried out at 1975°C for 5 hours.

3.6 Analysis of samples

After the densification and heat treatment the decomposed surface layer of all materials, were ground off and cleaned before further analysis.

3.6.1 Density measurements

The density of all the sintered and post-sintering heat-treated materials was measured using the Archimedes method. The first step was to measure the dry mass of the sample. The sample was then "boiled" in de-ionised water for one hour, under vacuum at room temperature. The water was then allowed to cool to room temperature. Using a wire basket apparatus, which allows the samples to be suspended in the water, the mass of the samples in water was measured. The sample was then taken out of the water and excess water was removed from the sample by dabbing it with a cloth. The mass of this "water-impregnated" sample was then measured.

The calculations for this method are briefly outlined in equations (3.5) and (3.6).

Bulk density (g/cm^3): $$\rho = \frac{d \times \rho_{H2O}}{(we - w)} \ . \qquad (3.5)$$

Open porosity (%): $$P_o = \frac{(we - d)}{(we - w)} \times 100\% . \qquad (3.6)$$

Where,

ρ_{H2O}= density of water at room temperature (ca. 20°C) = 0.9977g/cm^3,

d = dry mass of the sample,

w = mass of water-impregnated sample in water,

we= mass of water-impregnated sample.

3.6.2 X-ray diffraction phase analysis: qualitative and quantitative

The samples, powder, solid (sintered) and crushed (sintered), were scanned in a XRD7 Seifert-FPM, using Cu-Kα radiation with a Ni filter. For the Rietveld calculations, it was necessary to scan over a wide range of between 15° and 125°, for most measurements using a step-size of 0.02°, holding for 10 seconds per step. The quantitative phase analysis and the determination of the lattice parameter were made with the programme Autoquan (Seifert FPM) using the structural data given in the ICSD database.

The R_{wp}, or the "weighted profile R-value" can be defined as the mean weighted difference between the calculated diffraction pattern (fitted by a least squares approximation up to a best fit) and the measured XRD pattern. This parameter is calculated as shown in equation 3.7.

$$R_{wp} = \left[\frac{\sum w_i (y_{io} - y_{ic})^2}{\sum w_i y_{io}^2} \right]^{1/2}, \qquad (3.7)$$

where,

w_i = mass of component phase I,

y_{io}= intensity of experimentally observed XRD peaks for phase I,

y_{ic}= intensity of Rietveld calculated XRD peak for phase i.

Thus, R_{wp} is representative of the error in the result of the Rietveld calculation. A R_{wp} value of less than or equal to 10% was considered to

show a reasonably good (acceptable) agreement between experimental and calculated spectra.

The exact conditions under which the materials had to be run to obtain the lowest possible error, indicated by the "R_{wp}" value, was determined by first doing a series of calibration measurements. For these calibration measurements, a series of silicon carbide, alumina and YAG powders were mixed, XRD scans were performed on them and Rietveld calculations were done using these scan results. Tables of the powder mixtures are shown in Appendix A1.

Measurements and calculations were also done on the F1500 and F1200 powders (particle sizes 3μm and 10 μm respectively) because these are coarser than the UF15SiC powder (which was used to sinter all the materials in this project). This larger particle size resulted in narrower peaks, and therefore had less overlapping of the SiC polytypes, which results in the more easily reproducible determination of the polytypes. In particular, F1500 has a d50 particle size distribution of about 3.0 μm which is closer to what the expected mean particle size of the sintered and heat treated materials would be.

The rule of mixtures was used to calculate what the actual composition of the unsintered mixture was. The Rietveld refinement calculation results of these mixed powders were compared to the rule of mixtures calculation for the compositions of the mixtures. This was done to test the reliability of the Rietveld calculations in these powder systems. Some difference between the Rietveld- and the rule of mixtures-calculated results can be expected since error in the Rietveld calculations, due to extensive overlap of the SiC polytypes and grain boundary phase peaks, is inevitable. The results of this optimisation process are given in the Appendix A1.

The rule of mixtures was in reasonably good agreement with the Rietveld calculation results in most cases. It was therefore decided to use the following conditions for XRD scanning: 15-22°, 0.02^{o} step-size, 10 seconds per step for XRD scanning and calculation of all the sintered samples.

Initially solid surfaces of the sintered samples were scanned and calculated. The surfaces of hot pressed materials perpendicular and parallel to the direction of hot pressing were scanned and calculated and texture in 6H-SiC polytype was observed. In the GPS samples rich in YAG, apparent texture in the YAG phase was observed, probably because the YAG crystallites were large and so intensity results only from a very few grains, i.e the statistics of the measurement is not fulfilled, resulting in an apparent texture being observed. Because of these problems with apparent texture of the YAG phase, pieces of all HP, GPS and HT materials were crushed into powder for scanning and Rietveld calculation. After the crushing, the observed texture disappeared. Unless otherwise stated, all of the results of Rietveld calculations in secion 4.2, were done using scans of crushed sample powders.

3.6.3 X-ray Flourescence and ICP emission

XRF and ICP emission analysis done on one sample (HP-W3Y5Al) to check if there was any B contamination (from hBN coating of capsules, oxidation of the hBN was suspected) – the result was negative. If there was any boron or nitrogen contamination, it was below the limits detected by XRF and ICP emission techniques.

X-Ray Fluorescence was used to determine if there were any impurities in all the hot pressed and gas pressure sintered materials. Results are shown in section 4.2.

3.6.4 Microstructural analysis

Polishing

A small piece of samples was cut, embedded in resin and a cross-section polished with diamond suspensions down to a diamond particle size of to 1 μm. One of the problems encountered with the polishing was that SiC is a very hard material, therefore in order to remove scratches from the surface after grinding to a flat surface, long polishing times were required, when using diamond as a fine abrasive. The problem was that the grain boundary of the material (YAG phase and other phases resulting from the reaction between Y_2O_3 and Al_2O_3) is much softer than SiC, and therefore the long polishing times with the diamond caused "pull-out" of the softer grain boundary phases grains. This resulted in a nearly scratch-free material, which looked porous, but this apparent porosity was due to pull-out of the grain boundary grains-an artefact of the polishing. A polishing procedure used in the preparation is given in Appendix A2.

3.6.4.1 Optical light microscope investigation

Once the materials were polished, they were viewed under a light microscope in both dark and bright field modes.

3.6.4.2 Field Emission Scanning Electron Microscope (FESEM) investigation

Using the field emission scanning electron microscope in "back scatter mode", provides the imaging based on atomic number contrast. Since Y is much heavier than Si, this provides a good contrast between the Y-containing grain boundary phase and the Si-containing grain material.

Chemical etching was done by boiling samples in equal mass of KOH and $K_3Fe(CN)_6$ in water. The etching was reasonably successful (the results

are summarised in Appendix A, A3), however since the chemicals used were not very “friendly” and the study of cracks required that one see the grain and grain boundary material, it was decided to rather use the backscatter mode on the FESEM, than chemical etching for monitoring the microstructure.

Polished samples were cleaned ultrasonically in ethanol prior to viewing in FESEM and dried with a hair-drier. The samples, still mounted in insulative resin after polishing, had conducting carbon tape placed from the edges of the sample on two opposite sides, to the bottom of the sample, which was held by a metallic stub. In some cases this conducting path was not effective enough, and carbon dag was applied from the edges of the sample to the base of the metallic stub. The sample was then placed in the stage of the FESEM.

For the material being viewed in the FESEM, particularly for the purpose of image analysis, viewing conditions need to be optimised (to see the contrasting features of the microstructure). In the case of these LPSSiC optimised conditions used for all the samples were:

Table 3.11 FESEM parameters

Parameter	Setting
Applied voltage (keV)	7.0
Spot size	4.0
Scan	Single
Time	60 ms
Contrast	37.7
Brightness	45.0

Note that the contrast and brightness was changed slightly to give a set number (85%) in the threshholding used in the IMAGANALYSIS program. For the image analysis of a material, random positions were chosen and thirty images were taken along the points of a diagonal across the sample. Magnification was varied from sample to sample, depending on the grain size, so that a similar number of grains could be analysed from sample to

sample. The average number of grains analysed per sample was between 5000 and 7000.

A program for microstructural analysis was adapted for the liquid-phase sintered silicon carbide materials using the IMAGANALYSIS software package.The microstructural parameters calculated by the analysis program were:

i. SiC grain size distributions,
ii. Grain boundary distribution,
iii. SiC and grain boundary content,
iv. SiC Mean Free Path analysis,
v. Grain boundary Mean Free Path analysis,
vi. SiC contiguity.

The SEM micrograph images are in grey scale and the first step of the image analysis was to identify the certain range of grey colours, which corresponded to the phase of interest. Recall that the back-scatter detection mode was used to take the images, which allowed for good (grey-scale) contrast between the different phases. The grey scale in the range of interest was then assigned to be white and the remaining material was assigned to be black. This process of converting the grey scaling into the black and white colours only is known as “threshholding”.

At this point, an internally built module in the IMAGANALYSIS program separated the grains. Each grain area was measured in terms of pixels, and using a calibration factor, this area was converted into microns squared. The grain size distributions were calculated as follows. The area in microns squared was used to calculate an equivalent circular diameter that represents that particular area. This was done for each grain separately. Note that no calculations were done on grains cut by the edges of the image.

The data of the equivalent circular diameters of all the grains in a particular material, was then processed using a program in "Mathcad" software. The equivalent circular diameter values were first used to calculate back to the area of each grain. The total area was calculated by summing up areas of all the grains. "Bins" were created to divide the total area into segments. Fifty bins were used. The minimum and maximum grain size was identified and the difference between these two numbers was divided into 50 equal-sized bins. For example, bin number one was 0- 1μm, bin no. 2 was 1 – 2 μm, etc.

To calculate the number distribution, the total number of grains in each bin was calculated as a fraction of the total number of grains analysed. The area distribution was calculated by the total area in each bin. On the y-axis fraction % or area % was plotted versus grain size. The cumulative area distribution curve was obtained by summation of the bins.

The silicon carbide and grain boundary content were obtained by calculating the percentage area that each phase covered in the samples accumulatively.

The "Mean Free Path" of a phase in a material is defined as the average length of a phase before intercepting another phase. To measure this quantity, horizontal lines were drawn across the width of the image, with approximately 0.29 μm between lines in the lowest magnification used (2000X), and 0.058 μm between lines in the highest magnification used (10000X). These lines cover the whole length of the image. The segment of the line, which corresponds to the phase of interest, was measured in terms of length. The data of the silicon carbide and grain boundary phases was separated and analysed in terms of length over all the images, and the average determined was presented as the "Mean Free Path" for that phase.

Contiguity of silicon carbide in the liquid phase sintered material can be defined as the connectivity of the grains. This term is commonly used in the carbide industry to represent certain microstructures. This parameter is calculated by measuring the length of the silicon carbide grain peripheries, before the SiC grains are separated. Once the silicon carbide grains were separated, the SiC peripheries were measured again. The difference between these two quantities was multiplied by two (since a SiC contact would be measured once between two SiC grains). The percentage of this SiC –SiC connected length of the total periphery of the SiC grains was presented as the contiguity of the SiC grains, shown in equation 3.8 below.

$$\%\,\text{Contiguity} = 100 \times \left(\frac{2 \times \sum P_{SiC/SiC}}{2 \times \sum P_{SiC/SiC} + \sum P_{SiC/GB}} \right), \qquad (3.8)$$

where,

SiC refers to silicon carbide phase and GB refers to grain boundary phase,

$P_{SiC/SiC}$ = silicon carbide grains perimeter length before SiC grain separation,

$P_{SiC/GB}$ = silicon carbide to grain boundary interface length,

$P_{SiC/SiC} + P_{SiC/GB}$ = Total interface length after grain separation.

Separation of silicon carbide grains was difficult in many samples because of their intergrowth. This means that accurate determination of the SiC individual grain size distribution was not possible. However, trends in grain growth can be monitored by observing trends in the SiC mean free path. The trends in the calculated SiC mean free path were quantitatively in agreement with the trends observed in the calculated SiC mean grain size.

A lower magnification was used to analyse the heat treated materials, but the chosen magnification could not be too low, otherwise the finer grain size part of the distribution could not be analysed. This means that the

image analysis results of the SiC grain size of the HT4 materials (8 hour heat treatment at 1925°C) is not as accurate as that of the as-sintered and lower sintering time heat treatment materials (in which a more equiaxed, unimodal distribution was observed).

3.6.5 Mechanical properties

3.6.5.1 Vickers hardness and fracture toughness determination

Vicker's indentation hardness measurements were done using 10kg load. The diagonal lengths of the indentations (d1 and d2 in Figure 3.8 below) were used to calculate the hardness of the material (according to equation 3.9). The length of the cracks generated by the indentation (c1 and c2), were measured (as shown in Figure 3.8). and the crack lengths were used to calculate indentation fracture toughness of the materials, using equation 3.10.

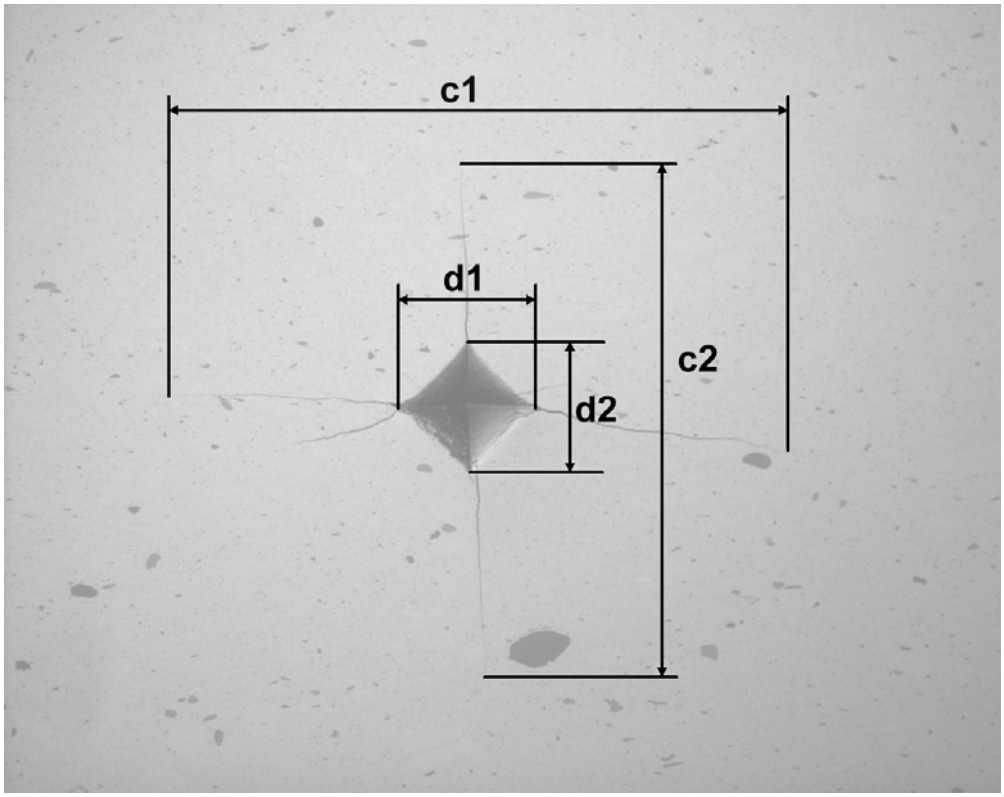

Figure 3.8 Figure indicating how the diagonals of the Vickers indentations and the crack lengths are measured

d1 = horizontal indentation length

d2= vertical indentation length

d= average indentation length

c1=horizontal length spanned by indentation cracks

c2= vertical length spanned by indentation cracks

c= average length spanned by indentation cracks

$$HV = \frac{\text{Applied load (kg)}}{\text{Contact area of indenter (mm}^2\text{)}}$$

$$= \frac{2P\sin\frac{\theta}{2}}{d^2}$$

$$HV = 1.85437\frac{P}{d^2} \qquad (3.9)$$

where,

HV = Vickers hardness number (kg/mm^2),

P = applied load (kg),

$\theta =$ angle between opposite faces (136° for Vickers diamond indenter),

d = diagonal of indentation (mm).

$$K_{1c} = 0.0316 \times K \times \left(\frac{E}{H \times 0.00981}\right)^{1/2} \times 98.1 \times \left(\frac{C}{1000}\right)^{-1.5} \quad , \quad (3.10)$$

where,

K= a prefactor , 0.020 for SiC,

E= elastic modulus (GPa),

H= Vickers hardness number (kg/mm^2),

C= radial crack dimension = c/2 (μm).

3.6.5.2 Four-point bending strength

In addition to hardness and fracture toughness, the four-point bending strength of the hot pressed and gas pressure sintered materials were measured. The materials were cut and the surfaces ground to make bending bars with dimensions 3.0 X 4.0 X 45 mm (European standard). After bending strength was determined, the fracture surface of certain lowest and highest bending strength materials, were studied using stereomicroscopy and SEM (fractographical study.)

Figure 3.9 shows an example of a fracture origin, which causes the material to fracture under high enough tensile stress and the fracture mirror surrounding it. In Figure 3.9, one can see that the two halves of the broken sample are exhibit fracture surfaces which are mirror images of each other and extend radially from the origin of fracture. This is the reason for this region (shown in the circle in Figure 3.9) being called the fracture mirror. Generally, a more circular fracture mirror in a broken sample indicates a fracture origin which is deeper in the sample. If one looks at the low magnification images of the failure origin and fracture mirror of most of the samples investigated in the study of the untempered HP bending bars, the mirrors are approximately semi-circular (illustrated in Figure 3.10).

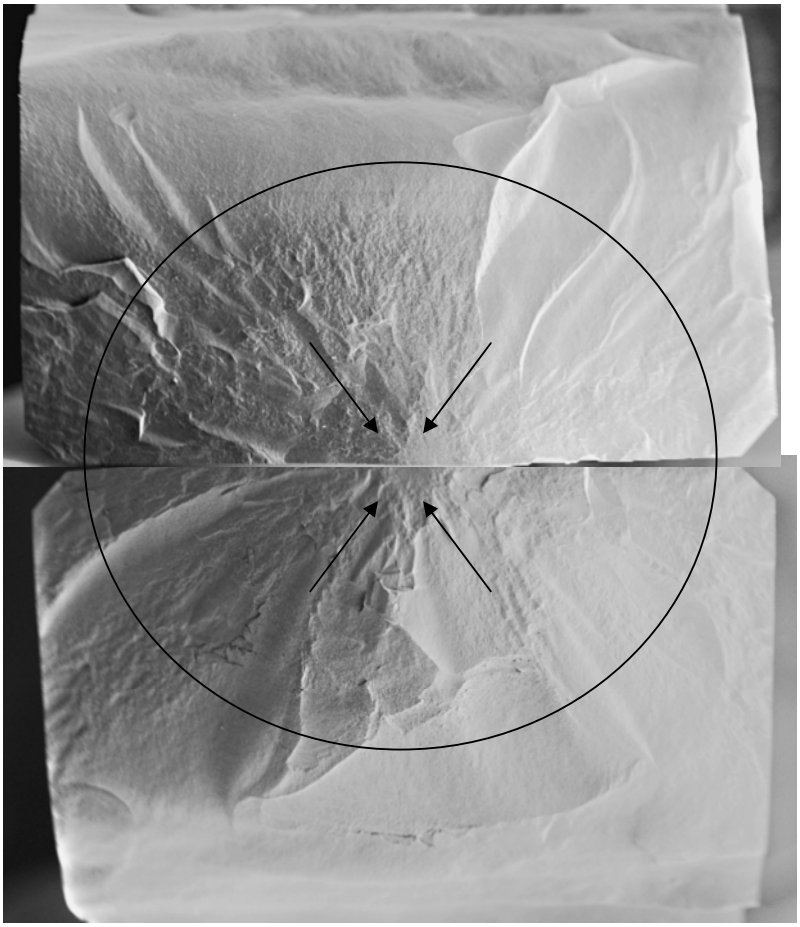

Figure 3.9 Fracture surfaces of broken HP4Y2AI bending bar (the arrows point to the fracture origin and the " fracture mirror" region is in the region of circle

This would imply that the origin of fracture is very close to the surface or indeed at the surface. This fact, together with the observations in the SEM investigations, shown in Figure 3.10, led to the conclusion that the failure origin in most of the as-ground (untempered) HP samples, were surface damage from the preparation of the samples.

In the microstructural study performed on the as-ground (untempered) HP bending bars, the samples tended to contain many larger SiC grains (about 5 -10 microns, compared to the mean grain size of 1 micron), these

larger grains were not large enough to be the cause of the failure, and were not found in the region of the origin of the failure of the material.

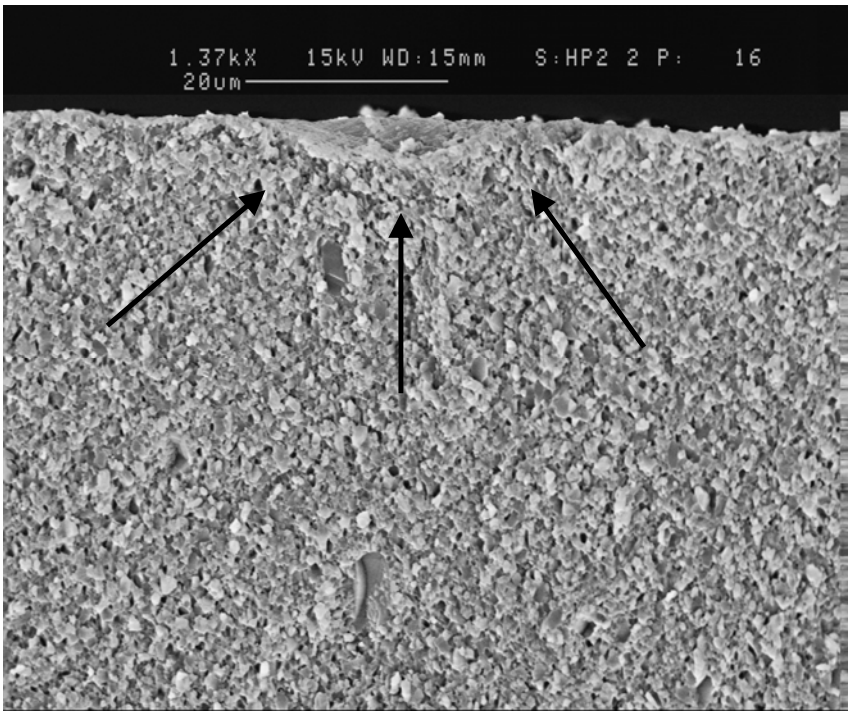

Figure 3.10 SEM micrograph of origin of failure region in HP4Y:2 AI .This is one example where surface damage is suspected to be the cause of failure

The further HP- and GPS-materials were tempered at 1250°C, for 2 hours in air, to heal surface defects from grinding, and the bending strength was repeated on these tempered hot pressed and gas pressure sintered bending bars. The bending strength of the tempered materials does not differ significantly from that of the untempered materials, but the fractographical study of the tempered materials, indicated fracture failure origin now to be due to some large SiC grains or porosity in the material.

3.6.5.3 Elastic modulus determination

The elastic modulus of the hot pressed, gas pressure sintered, heat treated and ultra-high pressure sintered materials was measured by applying ultrasonic pulses across the cross-section of the samples, using oil as a transmission medium.

The time that it took for the ultrasonic pulse to travel from the first surface s_1 to s_2 and then back again to s_1 was measured (see Figure 3.11). The thickness and density of each sample was then used to calculate the elastic modulus of each material, according to equation 3.11:

$$E = 2\left(\rho c_T{}^2\left(1+\left(\frac{t_T{}^2 - 2t_L{}^2}{2\left(t_T{}^2 - t_L{}^2\right)}\right)\right)\right), \qquad (3.11)$$

where,

E = elastic modulus ,

ρ = density of the material,

c_T = speed transverse wave

$= \frac{2d}{t_T}$,

t_T= time that it takes for transverse wave to move from the surface s_1 to s_2 and back to s_1,

t_L= time that it takes for longitudinal wave to move from the surface s_1 to s_2 and back to s_1, and

d= thickness of the sample.

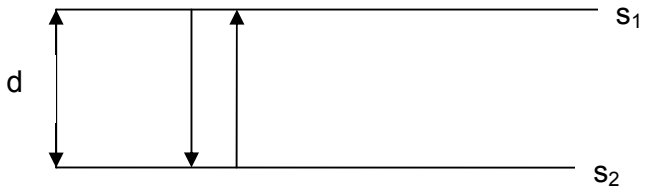

Figure 3.11 Schematic diagram to show parameters in elastic modulus determination

3.6.5.4 Crack resistance determination

In selected "HP-W" samples, crack resistance was measured by measuring Vicker's hardness at different loads. Three Vickers indentations were done for 1kg, 5kg, 10 kg on the new finish. The hardness and crack lengths were measured from the indents at different loads.

Graphs of the sum of crack lengths vs load were plotted and straight lines were obtained, the gradient of which is related to crack resistance of material. For the three as-sintered HP-W materials, no significant difference in crack resistance was observed. This crack resistance measurement was done on a cross-section (perpendicular to the direction of hot pressing) and a surface parallel to the direction of hot pressing.

3.6.5.5 Analysis of cracks propagating from Vicker's indentations

The cracks propagating from the Vicker's indentations were studied to determine which toughening mechanisms were most responsible for the toughening of that material.

For the purpose of these studies, SEM images of cracks of three indentations of the selected samples were taken, at 5000X magnification.

Of each indentation, 1 horizontal crack (in the case of hot pressed samples, perpendicular to the direction of hot pressing), and 1 vertical crack (in hot pressed samples, parallel to the direction of hot pressing), was analysed. Successive high magnification images were pasted in sequence to form the entire crack length, in the "Corel Draw" program. An example of such a crack is shown in Appendix A4. The program "Image Tool" was used to measure the length of the crack, and to determine the point where two thirds of the outer part of the crack started.

Three quantities were determined:

1) Crack roughness (ratio of total length of crack and "direct" length of the crack)
2) Ratio of intergranular to transgranular fracture per unit length
3) Number of crack bridges per unit length

These quantities were calculated for the outermost two thirds of the length of the crack.

3.6.6 Electrical properties

Four-point impedance spectroscopy was done using a *1610 Solartron Impedance Analyser.* The samples were also measured using a 2-probe *Novacontrol system.* All measurements were done in a rotary pump vacuum (8 mTorr). Electrical measurements were done over a frequency range 10^{-2} Hz – 1 MHz.

The samples which were to be measured by impedance spectroscopy were first cleaned ultrasonically in acetone and allow to dry in air. The larger faces were then painted with a ceramic gold paste (ca. 1000Å thick) using a paint brush. The samples were then heated up to 750°C (at a rate of 600°C per hour) and held at 750°C for 15 minutes. After this the

samples were allowed to cool down rapidly. This resulted in square parallel – plate capacitors.

The sample was then taken and placed within a load cell, which applies pressure to 4 wires (for the Solartron) or two wires (for the Novacontrol) so that these wires make direct contact with the gold-coated surface of the sample. This load cell was then placed inside a glass tube (for low temperature measurements), or a stainless steel furnace (for high temperature measurements.) The apparatus was then cooled using liquid nitrogen or heat treated, using a heating element. depending on the temperature of the measurement. When high temperature measurements were made, the measurement was first made at the highest temperature, and subsequent temperatures were measured as the apparatus was cooled to room temperature. No measurements were made until the temperature at which the measurement was to be made was completely stabilised. Measurements were repeated to ensure consistency and errors are estimated to be of order 1 %.

Measurements were made at 330°C, 300 ^{o}C , 250 ^{o}C , 200 ^{o}C, 150 ^{o}C, 100 ^{o}C, 50 ^{o}C, room temperature and –196°C (liquid nitrogen temperature). Particular temperatures were measured for each sample.

In the Impedance spectroscopy measurements made using two different apparatus: Novacontrol and Solartron, the default activation voltage was initially used for measurements. Later the activation voltages were set to be the same for both apparatus, because non-Ohmic behaviour was observed in some materials. Non-Ohmic behaviour was identified by a difference in current and phase measurement when the material was measured at different activation voltages.

The experimental Cole –Cole plot (Figure 3.12) below is a plot of negative imaginary impedance (-Z'') vs real impedance (Z'). As shown by the

arrows, extrapolating the semicircular arc to the x –axis gives the real impedance, or dc resistance of the phase, which is giving rise to that arc. This particular plot shows that if there is more than one phase in the material. Each arc allows one to distinguish the electrical properties of a particular phase(s) in the material. If there is only one arc or 1.5 arcs, this does not indicate that there is only one phase in the material, as other phases may have electrical properties, for example the frequency range, which is not accessible using the available instrumentation.

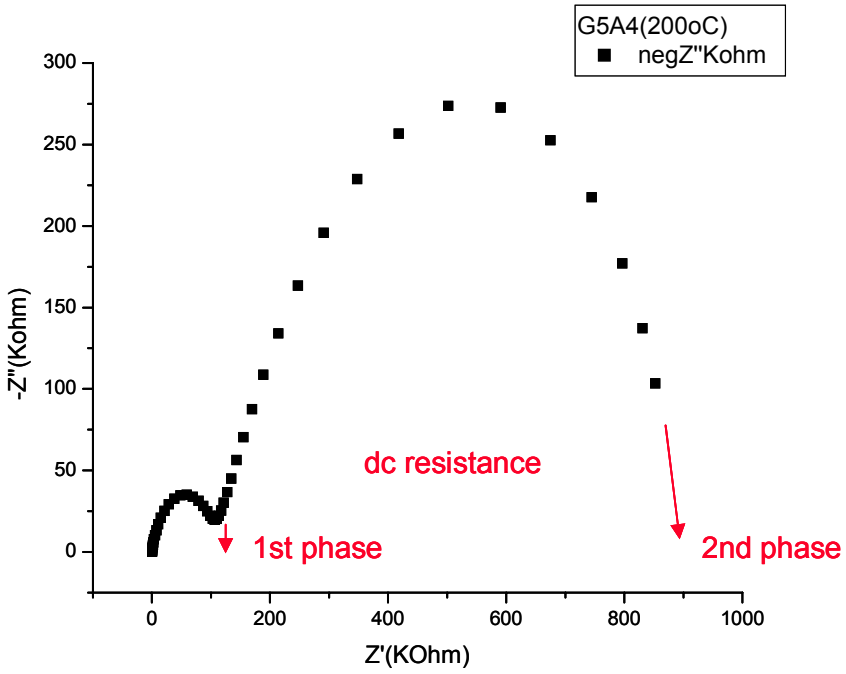

Figure 3.12 Cole-Cole plot for a Gas Pressure Sintered material (GP1Y4Al)

In the example given in Figure 3.12, the dc resistance of the first phase is about 150 KOhm, and the dc resistance of the second phase is approximately 750 KOhm.

Electrode effects are usually observed as a partial arc on the extreme right of a Cole-Cole plot, i.e. at low frequencies. In the case of the heat treated HP materials, partial arcs running in the negative x-direction, implying negative dielectric constants, were observed. This feature in the impedance spectra- observed only in the heat-treated materials, is due to some polarization effect at the electrodes (when a layer of charge carriers becomes trapped under the electrodes and cannot move)[185].

The peaks in the Cole-Cole plots are given by the peak frequency ω_c, i.e. the frequency which corresponds to the top of the impedance arc for that phase in the Cole-Cole plot. The peak frequency, ω_c, is the frequency at which the material changes from being primarily conducting material to being dielectric in behaviour. i.e. at frequencies below this, the material is conducting, and at higher frequencies exhibits dielectric behaviour. Along this line of reasoning, lower characteristic frequencies should then correspond to lower conductivities. ω_c is defined in equation 3.12 below.

$$\omega_c = \frac{\sigma}{\varepsilon_o \varepsilon_r} \qquad (3.12)$$

where,

σ is the conductivity,

$\varepsilon_o\varepsilon_r$ is the relative permittivity of the phase.

ε_o= the permittivity (dielectric constant) of free space (8.854×10^{-12})

ε_r= the dielectric constant of the phase.

An example of how the peak frequency for the different phases in a material can be determined by an Impedance plot, is given in Figure 3.13. This is a plot of negative real impedance vs log of the angular frequency.

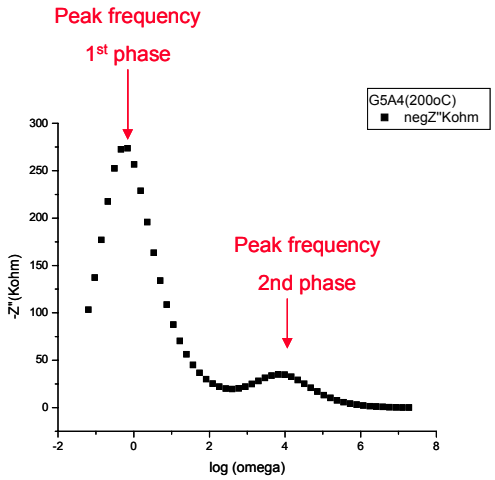

Figure 3.13 Plot to show characteristic frequency of two phases observed in the Cole-Cole plot in GP1Y4Al material

The frequency and dc resistance determined from the Cole-Cole plots were used to calculate the capacitance, C , according to equation 3.13,

$$C = \frac{1}{(\omega_c r)} \qquad (3.13)$$

where r is the dc resistance determined from the Cole-Cole plot.

The geometric factor, G, is defined as,

$$G = A/d \qquad (3.14)$$

where A = area of the paralleliped sample surface
T= thickness of the sample.

The capacitance and geometric factor of the samples was then used to calculate the dielectric constant ε, according to equation 3.15,

$$\varepsilon = \frac{C}{G\varepsilon_o} \qquad (3.15)$$

where ε_o = permittivity of free space (8.854×10^{-12})

Impedance spectroscopy done over a wide range of temperatures, can sometimes be used to determine the conduction mechanism. The conduction mechanism was determined from the exponent of the T in the Arrhenius type equation (2.27) on page 71.

Log conductivity was plotted against $1/T^n$, for various values of n, to determine the best linear fit. n = 1 corresponds to semiconductor conduction[197], n = 0.25 corresponds to 3-dimensional Mott variable range hopping, and n = 0.5 corresponds to variable range hopping with electronic interactions[191-196].

Excitation energies associated with the conduction mechanism were calculated from the best fit of equation 2.28, given on page 71.

In the impedance measurements of GPS 4 mass-%, SSiC, HT4HP1Y1Al and HT4HP1Y4Al, inconsistencies between the Novacontrol (2-point contact) and Solartron (pseudo 4-point contact) instruments, set at the same activation voltages, was observed (shown in Figure 3.14).

The Novacontrol and Solartron instruments should give similar results when set at the same activation voltages since they are both essentially 2-probe instruments. The Solartron is a vector voltmeter, whereas the Novacontrol instrument is a complex ac bridge-type system, which is essentially an ac version of the Wheatstone bridge system (i.e. balancing impedance and resistance). However, the Novacontrol cannot accurately measure resistances less than 1000 ohms, and the Solartron can in principle measure samples with low resistances (down to 1 ohm). The HT4 materials (hot pressed materials heat treated for 8 hours) are particularly very conducting. In the 3 most conducting HT4 materials, the Novacontrol measurement was consistently lower than the Solartron measurement, as shown in the figure below:

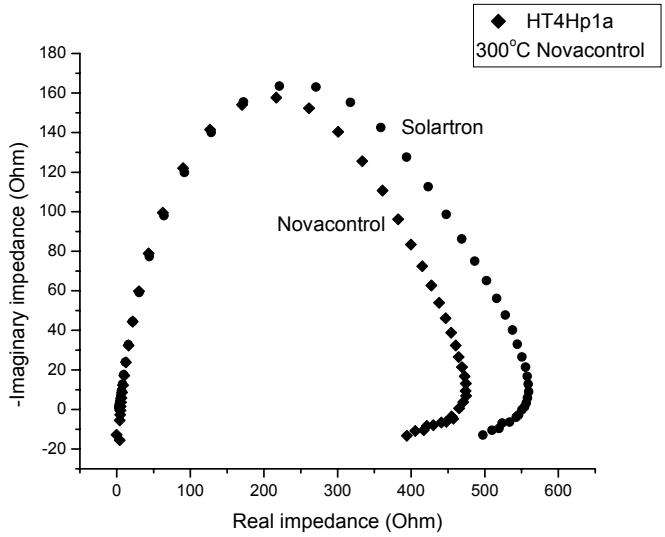

Figure 3.14 Cole-Cole plot of HT4HP3Y5Al, measured with the Novacontrol and Solartron at 300°C

In the lowest conductivity HT4 material, the high-Y_2O_3 containing material, in which segregation of grain boundary phase was observed on heat treatment of the hot pressed material (HT4HP4Y2Al), the Novacontrol and Solartron were in exact agreement at 300°C as shown in Figure 3.15.

This means that the Solartron is more reliable for all measurements below 1000 ohms, whereas Novacontrol results are more reliable in excess of 1000 ohms.

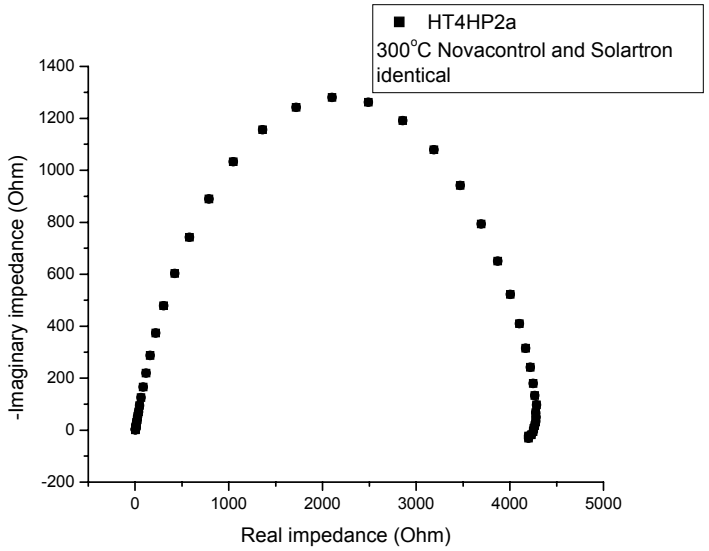

Figure 3.15 Cole-Cole plot of HT4HP4Y2Al, showing the identical Novacontrol and Solartron results at 300°C

3.7 Nomenclature of the samples

In the naming of the samples, the first letters denote the densification technique, namely hot pressing (HP), gas pressure sintering (GP) and ultra-high pressure sintering (UHP) and the remaining part gives information about the sintering additive Y_2O_3:Al_2O_3 mol ratio. A list of the sintered materials is given in Table 3.12. For example: GP3Y5Al, denotes a material which has been gas pressure sintered with sintering additives molar ratio of $3Y_2O_3$:$5Al_2O_3$.

All of the materials, with the exception of two materials in the Table 3.12 were sintered with 10 mass% Y_2O_3 and Al_2O_3 sintering additives, with different molar ratios of Y_2O_3 and Al_2O_3. The first exception is "HP1Y4Al_4", which, as the name indicates, denotes is a hot pressed material with $1Y_2O_3$:$4Al_2O_3$ molar ratio, but with 4 mass% sintering additives (instead of the standard 10-mass%). The second exception is

"HP0.7YS", which denotes a hot pressed material with 10 mass% sintering additives, which are $0.7Y_2O_3$:SiO_2.

Table 3.12 A summary of the sample nomenclature and conditions of preparation

Name	Densification technique/ heat treatment	Sintering additives content and molar ratio	Temperature (°C)	Time (hours)	Pressure
HP3Y5Al-W	Hot pressed*	$0.46Y_2O_3$:Al_2O_3	1900	0.5	36MPa, uniaxial
HP1Y1Al-W	Hot pressed*	$0.52Y_2O_3$:Al_2O_3	1900	0.5	36MPa, uniaxial
HP4Y2Al-W	Hot pressed*	$1.1Y_2O_3$:Al_2O_3	1900	0.5	36MPa, uniaxial
HP1Y4Al	Hot pressed**	$0.25Y_2O_3$:Al_2O_3	1925	0.5	30 MPa, uniaxial
HP3Y5Al	Hot pressed**	$0.6Y_2O_3$: Al_2O_3	1925	0.5	30 MPa, uniaxial
HP1Y1Al	Hot pressed**	$1Y_2O_3$: Al_2O_3	1925	0.5	30 MPa, uniaxial
HP4Y2Al	Hot pressed**	$2Y_2O_3$: Al_2O_3	1925	0.5	30 MPa, uniaxial
HP4Y1Al	Hot pressed**	$4Y_2O_3$: $1Al_2O_3$	1925	0.5	30 MPa, uniaxial
HP1Y4Al_4[1)]	Hot pressed**	$1Y_2O_3$: 4 Al_2O_3	1925	0.5	30 MPa, uniaxial
HP0.7YS	Hot pressed**	$0.7Y_2O_3$:SiO_2	1925	0.5	30 MPa, uniaxial
GP1Y4Al	Gas pressure sintered***	$1Y_2O_3$: 4 Al_2O_3	1925	1	80 bars, isostatic
GP3Y5Al	Gas pressure sintered***	$3Y_2O_3$: 5 Al_2O_3	1925	1	80 bars, isostatic
GP1Y1Al	Gas pressure sintered***	$1Y_2O_3$: $1Al_2O_3$	1925	1	80 bars, isostatic
GP4Y2Al	Gas pressure sintered***	$4Y_2O_3$: $2Al_2O_3$	1925	1	80 bars, isostatic

[1)] 4 mass-% sintering additives, otherwise all the other materials contain 10mass% sintering additives

* Hot pressing equipment used at Wits University: TTI (Thermal Technologies Inc. Astro, HP20 series)

** Hot pressing equipment used at IKTS: HPW200/250, KCE/FCT

*** Gas pressure sintering furnace

Hot pressed and gas pressure sintered materials which were heat treated are named with “HT” in front of the densification technique letters. The number after the HT gives information about the heat treatment cycle (i.e. post-sintering heat treatment time or temperature- see Table 3.13 for information).

For example: HT5HP3Y5Al indicates a hot pressed material of grain boundary composition $3Y_2O_3$:$5Al_2O_3$, which was then heat treated (HT5) for heat treatment cycle 5: 5 hours at 1975°C.

Table 3.13 A summary of the sample nomenclature for the post-sintering heat treated materials

Name	T (^{o}C)	Time (hours)	Pressure	Atmos-phere
HT2	1925	1.5	80 bars, gas pressure	Ar
HT3	1925	5	80 bars, gas pressure	Ar
HT4	1925	8	80 bars, gas pressure	Ar
HT5	1975	5	80 bars, gas pressure	Ar

In the case of the ultra-high pressure sintering used as the densification technique, in all cases external pressure applied during sintering was 5.5GPa and the samples were sintered for a few minutes. The ultra-high pressure sintered samples are divided into two groups. Table 3.14 contains a list of the ultra-high pressure sintered materials in the first group, in which the samples are named starting with the densification technique (UHP), followed by the sintering additive content (4 or 15mass%), and then the letter “R”, which stands for “run” and the given number of the sintering cycle.

Table 3.14 List of samples in group 1 sintered by ultra-high pressure sintering

Sample name	Y_2O_3:Al_2O_3 molar ratio	RUN no.	Approximate temperature* (°C)	Cooling
UHP4R1	0.25	1	1500	Very fast
UHP4R2	0.25	2	1550	Very fast
UHP4R3	0.25	3	1550	Slower
UHP4R4	0.25	4	1550	Even slower
UHP15R1	0.27	1	1500	Very fast
UHP15R2	0.27	2	1550	Very fast
UHP15R3	0.27	3	1550	Slower
UHP15R4	0.27	4	1550	Even slower

* exact temperature unknown because the furnace was power-controlled

In the second group UHP materials in Table 3.15, the "UHP" first denotes the densification technique, followed by the molar ratio of the Y_2O_3:Al_2O_3 (10 mass-%). An example of the first group is "UHP4R3", indicating a ultra-high pressure sintered material with 4 mass-% sintering additives, sintered under conditions of "Run 3" in Table 3.15. In group 2, "UHP3Y5Al" indicates a ultra-high pressure sintered material with 10 mass-%, $3Y_2O_3$:$5Al_2O_3$ molar ratio.

Table 3.15 Summary of 10 mass-% ultra-high pressure sintered materials

Sample name	Y_2O_3:Al_2O_3 molar ratio	RUN no.	Approximate temperature* (°C)	Cooling
UHP1Y4Al	1:4	3	1550	Slower
UHP3Y5Al	3:5	3	1550	Slower
UHP1Y1Al	1:1	3	1550	Slower
UHP4Y2Al	4:2	3	1550	Slower